THE JOURNAL OF BIOLOGICAL CHEMISTRY VOL. 286, NO. 13, pp. 11141–11154, April 1, 2011

Ncb5or Deficiency Increases Fatty Acid Catabolism and Oxidative Stress*[S]

Received for publication, October 20, 2010, and in revised form, January 27, 2011 Published, JBC Papers in Press, February 7, 2011, DOI 10.1074/jbc.M110.196543

Ming Xu[‡1], WenFang Wang[‡§¶1], Jennifer R. Frontera[§], Melanie C. Neely[‖], Jianghua Lu[**], Daniel Aires[§], Fong-Fu Hsu[‡‡], John Turk[‡‡], Russell H. Swerdlow[§§], Susan E. Carlson[‖], and Hao Zhu[‡§§¶¶2]**

From the Departments of [¶¶]Clinical Laboratory Sciences, [‡]Physical Therapy and Rehabilitation Science, [‖]Dietetics and Nutrition, [§]Internal Medicine-Dermatology Division, [**]Neurology, [§§]Biochemistry and Molecular Biology, and [¶]Pathology, The University of Kansas Medical Center, Kansas City, Kansas 66160 and the [‡‡]Department of Internal Medicine, Washington University School of Medicine, St. Louis, Missouri 63110

The endoplasmic reticulum-associated NADH cytochrome b_5 oxidoreductase (Ncb5or) is widely distributed in animal tissues. Ncb5or$^{-/-}$ mice develop diabetes at age 7 weeks and have increased susceptibility to the diabetogenic oxidant streptozotocin. Ncb5or deficiency also results in lipoatrophy and increased hepatocyte sensitivity to cytotoxic effects of saturated fatty acids. Here we investigate the mechanisms of these phenomena in prediabetic Ncb5or$^{-/-}$ mice and find that, despite increased rates of fatty acid uptake and synthesis and higher stearoyl-CoA desaturase (SCD) expression, Ncb5or$^{-/-}$ liver accumulates less triacylglycerol (TAG) than wild type (WT). Increased fatty acid catabolism and oxidative stress are evident in Ncb5or$^{-/-}$ hepatocytes and reflect increased mitochondrial content, peroxisome proliferator-activated receptor-γ coactivator 1α (PGC-1α) expression, fatty acid oxidation rates, oxidative stress response gene expression, and oxidized glutathione content. Ncb5or$^{-/-}$ hepatocytes readily incorporate exogenous fatty acids into TAG but accumulate more free fatty acids (FFA) and have greater palmitate-induced oxidative stress responses and cell death than WT, all of which are alleviated by co-incubation with oleate via TAG channeling. A high fat diet rich in palmitate and oleate stimulates both lipogenesis and fatty acid catabolism in Ncb5or$^{-/-}$ liver, resulting in TAG levels similar to WT but increased intracellular FFA accumulation. Hepatic SCD-specific activity is lower in Ncb5or$^{-/-}$ than in WT mice, although Ncb5or$^{-/-}$ liver has a greater increase in Scd1 mRNA and protein levels. Together, these findings suggest that increased FFA accumulation and catabolism and oxidative stress are major consequences of Ncb5or deficiency in liver.

NADH-cytochrome b_5 oxidoreductase (Ncb5or)[3] is an endoplasmic reticulum (ER)[4]-associated protein that has been implicated in lipid metabolism and diabetes. Ncb5or contains two redox domains that are homologous to cytochrome b_5 and its reductase (1) and a bridging domain that is a member of the CHORD-SGT1 (CS) protein family (2). The Ncb5or gene is found in all animals and is widely expressed among human and mouse tissues (1). Ncb5or-null (Ncb5or$^{-/-}$) mice develop diabetes at about 7 weeks of age due to loss of insulin-producing β-cells but maintain normal insulin sensitivity (3). The pro-apoptotic transcription factor C/EBP-homologous protein (CHOP) in the ER stress pathway appears to be involved in β-cell loss in Ncb5or$^{-/-}$ mice because CHOP deletion delays onset of diabetes by 2 weeks (4). Ncb5or$^{-/-}$ β-cells exhibit increased susceptibility to the diabetogenic effects of the oxidant streptozotocin *in vivo* (3) and *in vitro* (5). Furthermore, β-cells from 12-week-old (diabetic) Ncb5or$^{-/-}$ mice have mitochondrial hypertrophy and hyperplasticity (3). Ncb5or$^{-/-}$ mice also develop lipoatrophy independently of diabetes. Ncb5or$^{-/-}$ mice that receive islet transplants from wild-type (WT) mice at 7 weeks remain normoglycemic until age 12 weeks but still have greatly reduced triacylglycerol (TAG) stores, increased hepatic peroxisome proliferator-activated receptor-γ coactivator 1α (PGC-1α) expression, and a reduced monounsaturated fatty acid (MUFA) to a saturated fatty acid (SFA) ratio in hepatic TAG, diacylglycerols, and free fatty acids (FFA) (6). The loss of adiposity and the impaired fatty acid desaturation in Ncb5or$^{-/-}$ mice is similar to that seen in mice lacking stearoyl-CoA desaturase 1 (SCD1), which converts palmitic and stearic acids to palmitoleic and oleic acids, respectively (7). Ncb5or$^{-/-}$ hepatocytes are more sensitive than WT cells to palmitate-induced cytotoxicity, as reflected by ER stress marker expression and cell death (4, 6).

In vitro reconstitution experiments show that the Ncb5or homolog microsomal cytochrome b_5 (Cyb5A) and its cognate reductase Cyb5R3 provide electrons for the SCD reaction (8).

* This work was supported, in whole or in part, by National Institutes of Health Grants RO1-DK067355 (to H. Franklin Bunn and H. Z.) and in part by R01-HD047315 (to S. E. C.), RO1-AG022407 (to R. H. S.), R37-DK34388, P41-RR00954, P60-DK20579, and P30-DK56341 (to J. T.). Core facilities at the University of Kansas Medical Center were supported by NICHD, National Institutes of Health Grant HD02528.

[S] The on-line version of this article (available at http://www.jbc.org) contains supplemental Table 1 and Figs. 1–6.

[1] Both authors contributed equally to this work.

[2] To whom correspondence should be addressed: 3901 Rainbow Blvd., MSN 4048G-Eaton, KS City, KS 66160. Tel.: 913-588-2989; Fax: 913-588-5222; E-mail: hzhu@kumc.edu.

[3] Alternative designations for NADH- cytochrome b_5 oxidoreductase include Cyb5R4, b5/b5R, or b5+b5R.

[4] The abbreviations used are: ER, endoplasmic reticulum; DI, desaturation index; FAME, fatty acid methyl ester; FAO, fatty acid oxidation; FFA, free fatty acid; MUFA, monounsaturated fatty acid; SCD, stearoyl-CoA desaturase; SFA, saturated fatty acid; TAG, triacylglycerol; CHOP, C/EBP-homologous protein; OCR, oxygen consumption rate; DCF, dichlorofluorescin; PGC-1α, peroxisome proliferator-activated receptor-γ coactivator 1α; ACSL3, acyl-CoA synthetase-3; eIF, eukaryotic translation initiation factor; HMOX1, heme oxygenase 1.

Surprisingly, mice with global or hepatocyte-restricted Cyb5A deficiency exhibit only a mild deficiency of SCD products in hepatic lipids (9, 10), suggesting that another electron donor(s) may contribute to the SCD reaction *in vivo*. Ncb5or readily reduces a variety of artificial substrates *in vitro* in the presence of excess NADH or NADPH, as does the Cyb5A·Cyb5R3 complex (1, 11, 12). Ncb5or is a more potent electron donor than Cyb5A because of the lower redox potential ($E_0 = -108$ mV) in the Ncb5or heme center (11) and its unique heme environment (13). Of four recognized missense mutations in the human Ncb5or gene, two (Q187R and H223R) are found in a cohort with non-autoimmune diabetes (14). The other two (D371Y and L424M) occur at conserved residues in the b5R domain and are found as somatic mutations in 7% of human breast cancers (15). It is not yet known how these Ncb5or mutations affect its structure and function or contribute to disease pathogenesis.

To clarify the molecular bases of Ncb5or$^{-/-}$ cell hypersensitivity to cytotoxic effects of oxidants and of SFA and the potential role of Ncb5or in fatty acid desaturation, we have examined early molecular events and biochemical processes in the livers of prediabetic Ncb5or$^{-/-}$ mice at ages up to 5 weeks. We find that, starting early in neonatal development, livers of Ncb5or$^{-/-}$ mice exhibit increased expression of genes involved in uptake, synthesis, and desaturation of fatty acids and in mitochondrial biogenesis and oxidative stress responses. There are corresponding increases in mitochondrial content, fatty acid catabolism, and reactive oxygen species production. Ncb5or$^{-/-}$ hepatocytes incorporate fatty acids readily into TAG but accumulate more FFA and exhibit reduced content of MUFA relative to SFA at a given level of SCD expression, suggesting impaired SCD function. These defects in Ncb5or$^{-/-}$ cells appear to be responsible for their enhanced susceptibility to the cytotoxic effects of oxidants and palmitic acid.

MATERIALS AND METHODS

Animals, Diets, and Indirect Calorimetry—Ncb5or$^{-/-}$ mice were generated as previously described (3) and backcrossed into C57BL/6 for >12 generations. All experiments were performed in males as specified in a protocol approved by the Institutional Animal Care and Use Committee at the University of Kansas Medical Center. Ncb5or$^{-/-}$ and WT mice were generated from heterozygous crosses and maintained in a pathogen-free facility at 24 °C under a standard 12-h light/12-h dark cycle with free access to food and water. Standard rodent chow (Purina 5015 from LabDiet, St. Paul, MN) was used in all studies except the 10-day high fat diet feeding protocol in which the high fat diet (F5194 from BioServ, Frenchtown, NJ) was initiated immediately after weaning and continued for 10 days. The chow diet contains 3.8 kcal/g, 11% fat by weight, and a composition of 33% SFA, 35% MUFA, and 32% polyunsaturated fatty acids (PUFA), all of which in the form of TAG, in comparison to 5.1 kcal/g, 35% fat by weight with a composition of 40% SFA, 50% MUFA, and 10% PUFA in the high fat diet. Mice were sacrificed in the morning, and plasma and tissues were collected, flash-frozen in liquid nitrogen, and stored at −80 °C until use. Indirect calorimetry was conducted in a 4-chamber OxyMax System from Columbus Instruments (Columbus, OH). The O_2 and CO_2 gas fractions were monitored at both the inlet and output ports with a flow rate of 0.4 liter/min. These measurements were used to compute VO_2 and VCO_2 values (10 min per data point) in units of ml/kg/h. Respiratory exchange rate (RER) was calculated as VCO_2/VO_2 and used to predict the likely fuel source, *i.e.* RER = 1.0 (carbohydrates), 0.7 (fat), or 0.85 (proteins or a combination of carbohydrates and fats).

Electron Microscopy—Transmission electron microscopy was performed in the Electron Microscopy core facility at the University of Kansas Medical Center. Fresh liver pieces ~1 mm^3 in size were fixed in 2% glutaraldehyde in cacodylate buffer overnight before being processed and embedded in EPON. Micrographs were obtained with a JEOL (Tokyo, Japan) 100 CXII transmission electron microscope operated at 80 KV. The NIH Image J software was used for counting mitochondrial and cytoplasmic area.

Quantitative RT-PCR—Total RNA was prepared from livers or hepatocytes of WT and Ncb5or$^{-/-}$ mice using TRIzol reagent according to manufacturer's instructions (Invitrogen). RNA was assessed by determining absorbance of UV light at 260 and 280 nm wavelengths, with A_{260} for quantity and A_{260}/A_{280} ratio for quality. Two μg of RNA were reverse-transcribed to cDNA with Moloney murine leukemia virus (Invitrogen), and Power SYBR Green PCR Master Mix (Applied Biosystems, Foster City, CA) was used for quantitative PCR. Reactions, 10 μl each in a 384-well, were performed in duplicate for 40 cycles according to a 2-step protocol (92 °C for 15 s and 60 °C for 1 min) on a Prism 7900 Sequence Detection System (Applied Biosystems). The amount of target mRNA was calculated with the comparative C_T method and then normalized to that of 18 S rRNA. Primer Express 2.0 was used to design primers that span introns. Primer sequences are available upon request.

Mitochondrial DNA Content—Quantitative PCR was performed as above to determine the relative copy numbers of mitochondrial DNA (mtDNA) and nuclear DNA (nDNA) in livers from 5-week-old WT and Ncb5or$^{-/-}$ mice. Each reaction (10 μl) contained genomic DNA (100 ng) and forward and reverse primers (0.6 μM each). Hexokinase 2 (intron 9) and 16 S rRNA were used as nDNA- and mtDNA-specific targets, respectively, as described (16). A standard dilution series was used to confirm the efficiency of exponential amplification for each primer pair. The mitochondrial to nuclear DNA ratio in each sample was calculated by dividing the value for 16 S by that for hexokinase 2.

Immunoblot Analysis—Small pieces (~50 mg) of mouse livers were homogenized in lysis buffer (25 mM HEPES, 50 mM KCl, 6% glycerol, 5 mM EDTA, 5 mM EGTA, 0.5% Triton X-100, 50 mM NaF, 40 mM glycerol phosphate, and 25 mM sodium pyrophosphate) with inhibitors of phosphatases (PhosSTOP from Roche Applied Science) and proteases (SigmaFAST from Sigma). The lysate was then cleared by centrifugation (16,000 × *g*, 10 min, 4 °C). Total protein content was determined with Coomassie Plus reagents (Pierce). Proteins (~50 μg) were loaded into each lane on a 4–15% gradient SDS-PAGE gel. After electrophoresis, each gel was blotted onto a nitrocellulose membrane (GE Healthcare) and subjected to immunoblotting with primary antibodies against total and phosphorylated eIF2α (Cell Signaling Technology, Danvers, MA), PGC-1α

(Calbiochem), SCD1 (Santa Cruz Biotechnology, Santa Cruz, CA), and GAPDH (Sigma). Signals were developed with horseradish peroxidase-conjugated secondary antibodies and Super-Signal West Pico chemiluminescent substrate (Pierce). The Adobe Photoshop software was used to quantify intensity of signals.

Lipid Profiling and Total Content Assay—Frozen liver tissues (50–100 mg) or hepatocytes (5×10^5) were homogenized in lysis buffer (18 mM Tris-HCl, 50 mM EGTA, 300 mM mannitol, pH 7.5, 1 mM phenylmethanesulfonyl fluoride). Internal standards consisting of heptadecanoic acid (C17:0) and corresponding to each class of lipid species of interest was added at this step for quantification. Total lipids in liver homogenate or plasma (100–200 μl) were extracted by the method of Folch *et al.*(17) using chloroform and methanol (2:1) that contained 0.1% butylhydroxytoluene to prevent lipid oxidation. TAG and FFA were separated by TLC on silica gel plates using a solvent system of hexane:diethyl ether:acetic acid (80:20:1), and the separated classes were recovered from the plates and subjected to transmethylation as described (18). Fatty acid methyl esters (FAMEs) of liver and hepatocyte lipid samples were analyzed by GC-FID on a GC3900 with flame ionization detector (FID) or by GC-MS on a GC450 with MS220, respectively, from Varian (Palo Alto, CA). Both systems used a 100 m × 0.25-mm column, either Supelco SP-2560 with GC3900 or Varian FAME Select CP 7420 with GC450. Supelco 37 component FAME mix standards (Sigma) were used to confirm the identity of all FAMEs. The absolute amount in each FAME was calculated against the C17:0 internal control by comparing their peak areas (flame ionization detector) or total ion current where 10 specific and abundant ions of each FAME species were counted and the sum was divided by a response factor to generate its total ion current. Total tissue weight (livers) or protein content (hepatocytes) was used to normalize lipid content. For assay of total content of TAG, nonesterified fatty acid, free cholesterol, cholesterol ester, and total lipids from livers or plasma (without internal standard) were resuspended with 10% Triton X-100 in isopropyl alcohol and measured by colorimetric kits from Sigma or Wako Chemicals (Richmond, VA).

Isolation of Hepatocytes, Fatty Acid Treatment, and Cell Viability Assay—Hepatocytes were isolated from 4-week-old Ncb5or$^{-/-}$ and WT mice that were fasted for 2 h by using a 2-step perfusion procedure with Solution I (0.5 mM EGTA and 5.5 mM glucose in Hanks' buffered salt solution) and Solution II (1.5 mM $CaCl_2$, 5.5 mM glucose, with 0.0375% collagenase) as modified from (19). Live hepatocytes with survival rates of 85–90% were incubated in Williams' medium E (Invitrogen) containing 10% fetal bovine serum (FBS), glutamine, and penicillin/streptomycin at 37 °C overnight before an 8-h fatty acid treatment with bovine serum albumin (BSA)-complexed palmitic acid (C16:0) or oleic acid (C18:1), or BSA carrier alone. To avoid non-physiological toxic effects of fatty acids, each stock solution was prepared by complexing fatty acids (final concentration 5 mM) with 2.1 mM fatty acid-free BSA in 0.1 M Tris-HCl, pH 8.0, with constant stirring under nitrogen at 37 °C overnight, resulting in a molar FFA:BSA ratio of 2.4:1 (20). Solutions were then passed through a filter (0.2 μm) and stored at −80 °C until use. Fatty acid concentrations were measured with a non-esterified fatty acid C kit (Wako Chemicals). All reagents were purchased from Sigma unless otherwise indicated. The viability of cells was determined from their measured ATP content (CellTiter-Glo(R) Luminescent Cell Viability Assay kit, Promega, Madison, WI).

Ceramide Analyses—After fatty acid treatment, hepatocytes from each 6-cm plate were rinsed with isotonic LiCl before lipid extraction by the method of Bligh and Dyer (21). Ceramide (CM) species were measured to C8:0-CM internal standard by negative ion electrospray ionization/MS as previously described (22) and normalized to sample protein content.

Fatty Acid Oxidation (FAO)—The rate of mitochondrial FAO was calculated by measuring the oxidized product of [n9,10-^{3}H]palmitic acid (Perkin Elmer Life Science) as described (23). Briefly, 1×10^5 hepatocytes were seeded in wells of a 24-well plate, incubated overnight in medium with 10% FBS, and then incubated (2 h, 37 °C) with BSA-complexed palmitic acid (0.125 mM unlabeled plus 0.08 μCi of [n9,10-^{3}H]C16:0) in the presence of carnitine (1 mM) in PBS. The amount of substrate taken up by cells within 2 h represented less than 25% that of the total amount in the medium. The H[^{3}H]O product was collected, and its ^{3}H content was determined by liquid scintillation spectrometry (LS6500 Scintillation Counter, Beckman-Coulter, Brea, CA) to calculate the initial reaction rate (mmol/h/mg of protein). The protein contents of cells were measured with a BCA protein analysis kit (Pierce).

Extracellular Flux Analysis—Extracellular flux analysis was performed on a XF24 analyzer (Seahorse Bioscience, Billerica, MA) as previously described (24). Briefly, 3×10^4 hepatocytes were seeded into 24-well plates and cultured overnight in complete medium with 10% FBS (see above). Cells were washed with DMEM (0.8 mM $MgSO_4$, 1.8 mM $CaCl_2$, 143 mM NaCl, 5.4 mM KCl, 0.91 mM NaH_2PO_4, 15 mg/ml phenol red, 5.5 mM glucose, and 2 mM GlutaMAX from Invitrogen) and incubated in the same medium (37 °C, 1 h without CO_2 preincubation). Cells were then loaded into the XF24 analyzer to measure oxygen consumption rate (OCR) in short and repeated intervals as cells alone (base line) and after injection with buffer or BSA-complexed palmitic acid or oleic acid (0.125 mM) in the presence of carnitine (1 mM). OCR values under each condition were normalized to total protein content.

Measurement of Glutathione—Reduced and oxidized glutathione in liver tissue or hepatocytes were measured as described (25). Briefly, hepatocytes were washed with ice-cold phosphate-buffered saline (PBS) and then collected in ice-cold 3% sulfosalicylic acid, 0.1 mM EDTA. Similarly, frozen liver tissue was homogenized in 3% sulfosalicylic acid before centrifugation (16,000 × *g*, 5 min, 4 °C) to remove proteins. Pellets were dissolved in 10% SDS for protein determination as above, and the supernatant was divided into aliquots to measure total and oxidized glutathione. For the latter, GSH was derivatized with *N*-ethylmaleimide (Sigma), and the solution was passed through a Sep-Pak C18 cartridge (Waters, Milford, MA). Thiol contents of the total and GSSG aliquots were measured by mixing with Solution 1 (1.2 mM 5,5′-dithiobis-2-nitrobenzoic acid or 30 mM EDTA, 0.08% BSA, 600 mM potassium phosphate, pH 7.2) and Solution 2 (0.5 mg/ml NADPH, 2.5 units/ml glutathione reductase in 100 mM imidazole, pH 7.2, 2 mM EDTA, 0.04%

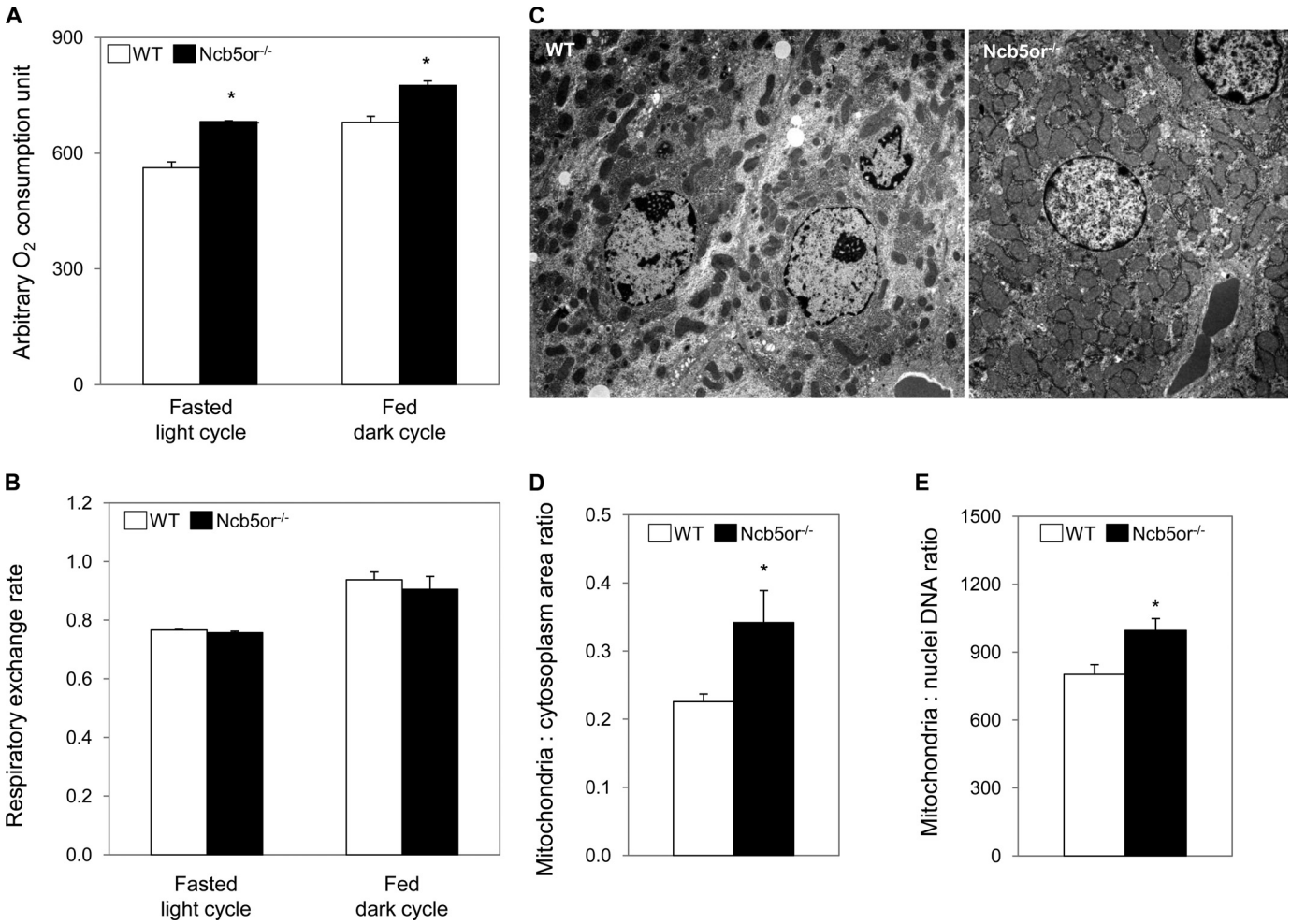

FIGURE 1. **Whole body O_2 consumption and respiration exchange ratio, and hepatic mitochondrial content of chow-fed Ncb5or$^{-/-}$ and WT mice.** *A*, O_2 consumption of 5-week-old Ncb5or$^{-/-}$ and WT mice was measured by indirect calorimetry and plotted as a function of time. The area under the *bar* was calculated for each mouse during light (fasting) or dark (fed) cycle. *B*, respiration exchange ratio of CO_2 production *versus* O_2 consumption of each mouse was calculated for each time point and averaged for the entire light (fasting) or dark (fed) cycle. Results in *A* and *B* were obtained from 3 pairs ($n = 3$) and plotted as the mean ± S.E. *C*, representative transmission electron microscopy of WT and Ncb5or$^{-/-}$ hepatocytes at 5 weeks of age are shown. *D*, the mitochondrial and cytoplasmic area was counted by the NIH ImageJ software and used to calculate the mitochondria:cytoplasm area ratio. A total of three pairs ($n = 3$, >10 cells per animal) were analyzed, and results are expressed as the mean ± S.E. *E*, ratios of mitochondria:nuclei DNA (16 S rRNA:hexokinase 2) were determined by quantitative PCR. A total of seven pairs ($n = 7$) were analyzed, and results are expressed as mean ± S.E. *, $p < 0.05$. *White bar*, WT; *black bar*, Ncb5or$^{-/-}$.

BSA). The cycling reaction was complete after 10-min of incubation at room temperature, and the GSH-reduced products (5-thio-2-nitrobenzoic acid) were measured by A_{412}. Levels of free thiol were determined relative to a GSH standard calibration curve.

Measurement of Cellular Hydrogen Peroxide—Cellular hydrogen peroxide and nuclear DNA levels were determined by staining with 2′,7′-dichlorofluorescin diacetate (Sigma) and Hoechst 33342 (Molecular Probes, Eugene, OR), respectively. After washing with PBS, cells were incubated (37 °C for 20 min in the dark) with 2 μM 2′,7′-dichlorofluorescin diacetate and 0.1 μg/ml Hoechst in Hanks' buffered salt solution (with Ca^{2+} and Mg^{2+} but without phenol red). Cells were collected by trypsinization and resuspended in PBS plus 20 mM glucose at a density of 1×10^6 cells/ml. Fluorescence measurements were performed in clear 96-well plates with excitation/emission wavelengths of 480/533 nm (DCF) or 355/460 nm (Hoechst) on a SpectraMax M5 microplate reader (Molecular Devices, Sunnyvale, CA). Cellular hydrogen peroxide level was normalized to nuclear DNA content as represented by the DCF:Hoechst ratio.

SCD Assay—SCD activity was determined by using [^{14}C]stearoyl-CoA (American Radiolabeled Chemicals, St. Louis, MO) as described (26). Briefly, microsomes were isolated from mouse livers and purified on a continuous density gradient (11). Fifty μg of microsomal proteins were mixed with 2 nmol of [^{14}C]stearoyl-CoA and 1 μmol of NADH in 0.1 mM Tris-HCl, pH 7.0, and incubated (37 °C, 5 min). Total lipids were extracted and transmethylated as above to yield FAME. Radiolabeled substrates (C18:0) and products (C18:1) were separated by TLC on silica gel plates containing 10% $AgNO_3$ (Analtech, Newark, DE). Signals were stored with phosphorimaging and quantitated with a Molecular Imager Pro Plus system with Quantity One software (Bio-Rad). Counts were used to calculate the yield ((C18:1)/(C18:0 + C18:1)), which was then converted to SCD activity (nmol/min/mg). All reactions were linear within the first 15 min under the above conditions.

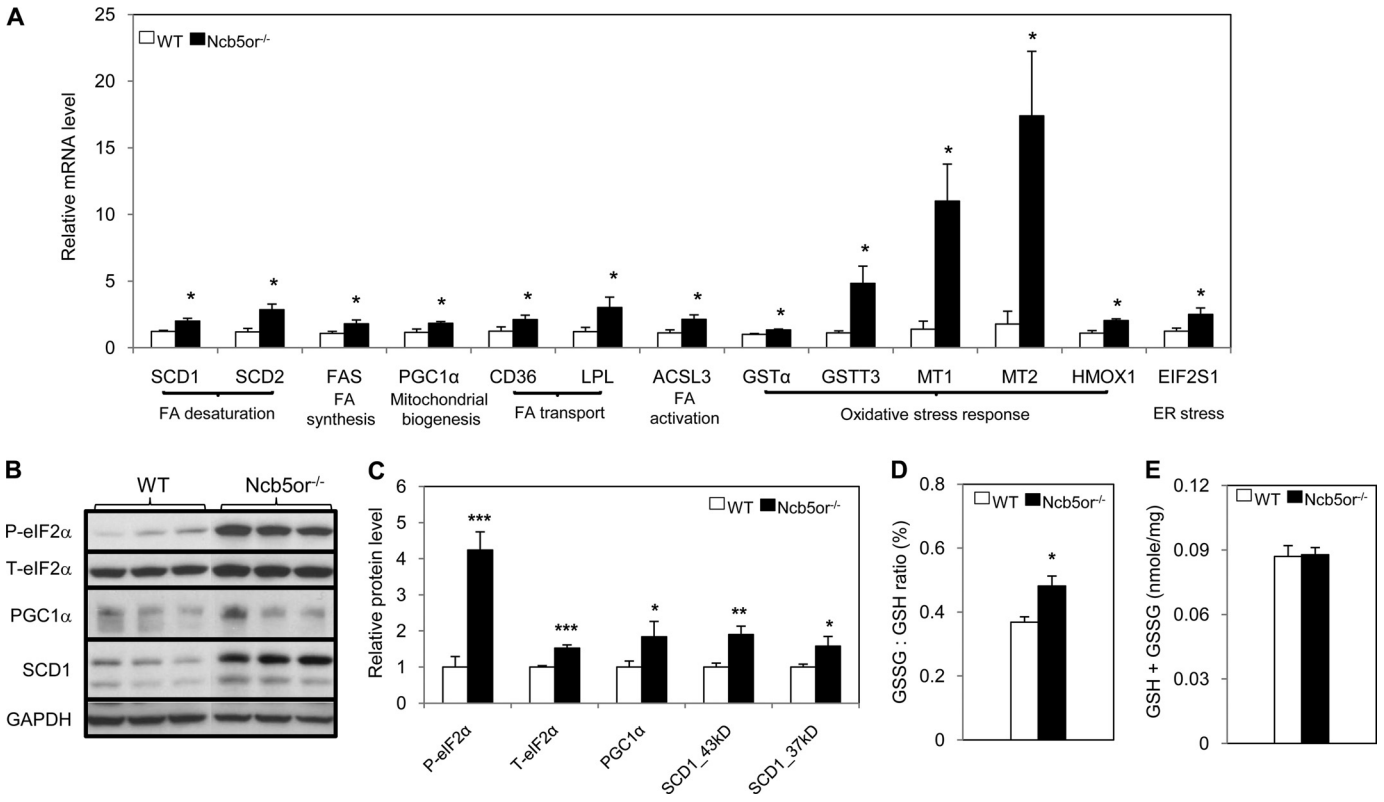

FIGURE 2. **Oxidative stress markers and lipid metabolism in chow-fed Ncb5or$^{-/-}$ and WT mouse liver tissue.** *A*, the relative mRNA levels of genes in oxidative stress and lipid metabolism in WT and Ncb5or$^{-/-}$ RNA samples are shown. The level of averaged WT sample was arbitrarily defined as 1 to allow comparison for each target gene. Six pairs of WT and Ncb5or$^{-/-}$ samples ($n = 6$) were compared. *FA*, fatty acid. *B*, immunoblotting analysis for phosphorylated (*P-*) and total (*T-*) eIF2α, SCD1, PGC-1α, and GAPDH in WT and Ncb5or$^{-/-}$ liver lysate. Relative intensities against GAPDH (loading control) were calculated from 4 pairs ($n = 4$) and plotted in *C*. Intracellular GSSG and GSH levels of six pairs of liver samples were measured ($n = 6$) and shown as the GSSG:GSH ratio in *D* and GSH + GSSG (total glutathione content) in *E*. All results were obtained from 5-week-old mice and are expressed as the mean ± S.E. *, $p < 0.05$; **, $p < 0.01$; ***, $p < 0.005$. *White bar*, WT; *black bar*, Ncb5or$^{-/-}$.

Statistical Analyses—Statistical analyses were performed with one-way analysis of variance. p values of <0.05 were considered statistically significant. Values are presented as the means ± S.E.

RESULTS

Increased Oxygen Consumption and Mitochondrial Density in Ncb5or$^{-/-}$ Mice—Lower body weights and loss of adiposity are observed in chow-fed Ncb5or$^{-/-}$ mice at ages 6 weeks and older (6). Here we report that despite similar body weights at birth, Ncb5or$^{-/-}$ mice exhibited significantly lower body weights than WT littermates as early as 2 weeks of age (supplemental Table 1).

To determine whether increased oxidative metabolism (catabolism) retarded growth in Ncb5or$^{-/-}$ mice, whole body oxygen consumption of 5-week-old animals was examined by indirect calorimetry. As expected, all mice consumed more oxygen during fed cycles compared with fasting intervals, but Ncb5or$^{-/-}$ mice consumed significantly more O_2 than WT mice by 21 and 14% during fasting and fed periods, respectively (Fig. 1*A*). This reflects a profound change in whole body substrate utilization. No significant difference in respiration exchange ratios was observed (Fig. 1*B*), suggesting the two genotypes oxidized similar substrate classes.

Consistent with increased oxidative metabolism in Ncb5or$^{-/-}$ mice, the density of mitochondria per unit cytosolic area was significantly higher in Ncb5or$^{-/-}$ than WT hepatocytes at age 5 weeks, as shown by transmission electron microscopy (Fig. 1, *C* and *D*). We also observed a significantly higher mitochondrial to nuclear DNA ratio in livers from Ncb5or$^{-/-}$ compared with WT mice by quantitative PCR (Fig. 1*E*), but no difference in mitochondrial density was observed at 2 weeks (supplemental Fig. 1) when the body weights of Ncb5or$^{-/-}$ mice first began to diverge significantly from WT.

Altered Fatty Acid Metabolism and Increased Oxidative Stress in Ncb5or$^{-/-}$ Livers—Microarray analyses of liver RNA samples from mice at age 5 weeks indicated that genes in the following metabolic and stress response pathways are up-regulated in Ncb5or$^{-/-}$ compared with WT mice, which was further confirmed by quantitative RT-PCR (Fig. 2*A*): 1) mitochondrial biogenesis (PGC-1α (27)), 2) fatty acid desaturation (SCD1 and SCD2 (28, 29)), 3) fatty acid synthesis (fatty acid synthase (30)), 4) fatty acid uptake (lipoprotein lipase and Cluster of Differentiation 36 (31, 32)), 5) fatty acid activation (long chain acyl-CoA synthetase-3 (ACSL3) (33)), 6) oxidative stress response (glutathione *S*-transferase isoforms (GSTa and GSTT3) (34), metallothionein isoforms (MT1 and MT2) (35, 36) and heme oxygenase 1 (HMOX1) (37)), and 7) ER and redox stress responses (eukaryotic translation initiation factor 2 (eIF2s1/eIF2α) (38)).

TABLE 1

Transcript levels of genes involved in lipid metabolism, mitochondrial biogenesis, and oxidative stress responses in newborn, 2-, 3-, and 5-week-old Ncb5or$^{-/-}$ and WT mouse livers

All values are the mean ± S.E. ($n = 6$) and relative to 18 S ($\times 10^6$). FAS, fatty acid synthase; LPL, lipoprotein lipase.

	Newborn		2 Weeks		3 Weeks		5 Weeks		
	WT	Ncb5or$^{-/-}$	WT	Ncb5or$^{-/-}$	WT	Ncb5or$^{-/-}$	WT	Ncb5or$^{-/-}$	Fold ↑ Ncb5or$^{-/-}$
SCD1	59.0 ± 7.7	134 ± 22[a]	8.64 ± 1.38	19.2 ± 2.9[a]	394 ± 51	222 ± 74	725 ± 58	1410 ± 140[a]	1.9
SCD2	41.1 ± 5.1	131 ± 23[a]	4.06 ± 0.43	5.74 ± 0.95	4.09 ± 0.55	5.25 ± 0.55	1.57 ± 0.35	3.79 ± 0.58[b]	2.4
FAS	5.90 ± 1.11	12.5 ± 2.9[a]	3.10 ± 0.51	5.10 ± 0.72[b]	30.9 ± 2.9	20.4 ± 6.3	16.8 ± 2.5	27.9 ± 3.9[b]	1.7
PGC-1α	28.5 ± 3.9	34.6 ± 1.9	15.7 ± 2.7	21.0 ± 4.2	11.6 ± 2.6	32.0 ± 5.5[c]	6.24 ± 1.17	11.3 ± 0.8[b]	1.8
ACSL3	0.94 ± 0.13	1.92 ± 0.32[b]	0.93 ± 0.10	2.31 ± 0.39[a]	2.04 ± 0.21	1.76 ± 0.39	1.88 ± 0.34	3.73 ± 0.58[b]	2.0
CD36	22.8 ± 3.9	15.5 ± 1.5	5.28 ± 0.62	6.64 ± 0.98	5.78 ± 0.95	10.6 ± 0.7[c]	4.76 ± 1.03	9.20 ± 1.52[c]	1.9
LPL	105 ± 9	114 ± 23	170 ± 22	138 ± 11	66.8 ± 11.0	209 ± 22[a]	15.4 ± 2.9	37.3 ± 8.8[b]	2.5
MT1	1061 ± 85	1576 ± 136[b]	94.5 ± 16.1	286 ± 93[b]	273 ± 62	394 ± 102	9.52 ± 2.74	93.8 ± 17.6[a]	9.9
MT2	249 ± 37	362 ± 47	15.5 ± 3.1	50.6 ± 19.9	56.6 ± 13.7	90.6 ± 12.8	1.02 ± 0.38	14.7 ± 3.6[a]	14
HMOX1	26.8 ± 4.7	23.3 ± 1.7	4.86 ± 0.86	12.6 ± 2.5[b]	11.6 ± 0.6	14.7 ± 1.4	2.48 ± 0.44	5.00 ± 0.30[a]	2.0
GSTT3	2.61 ± 0.27	2.70 ± 0.22	2.55 ± 0.30	4.12 ± 0.53[b]	7.12 ± 1.01	6.37 ± 1.41	3.49 ± 0.84	7.42 ± 2.21[b]	2.1

[a] $p < 0.005$.
[b] $p < 0.05$.
[c] $p < 0.01$.

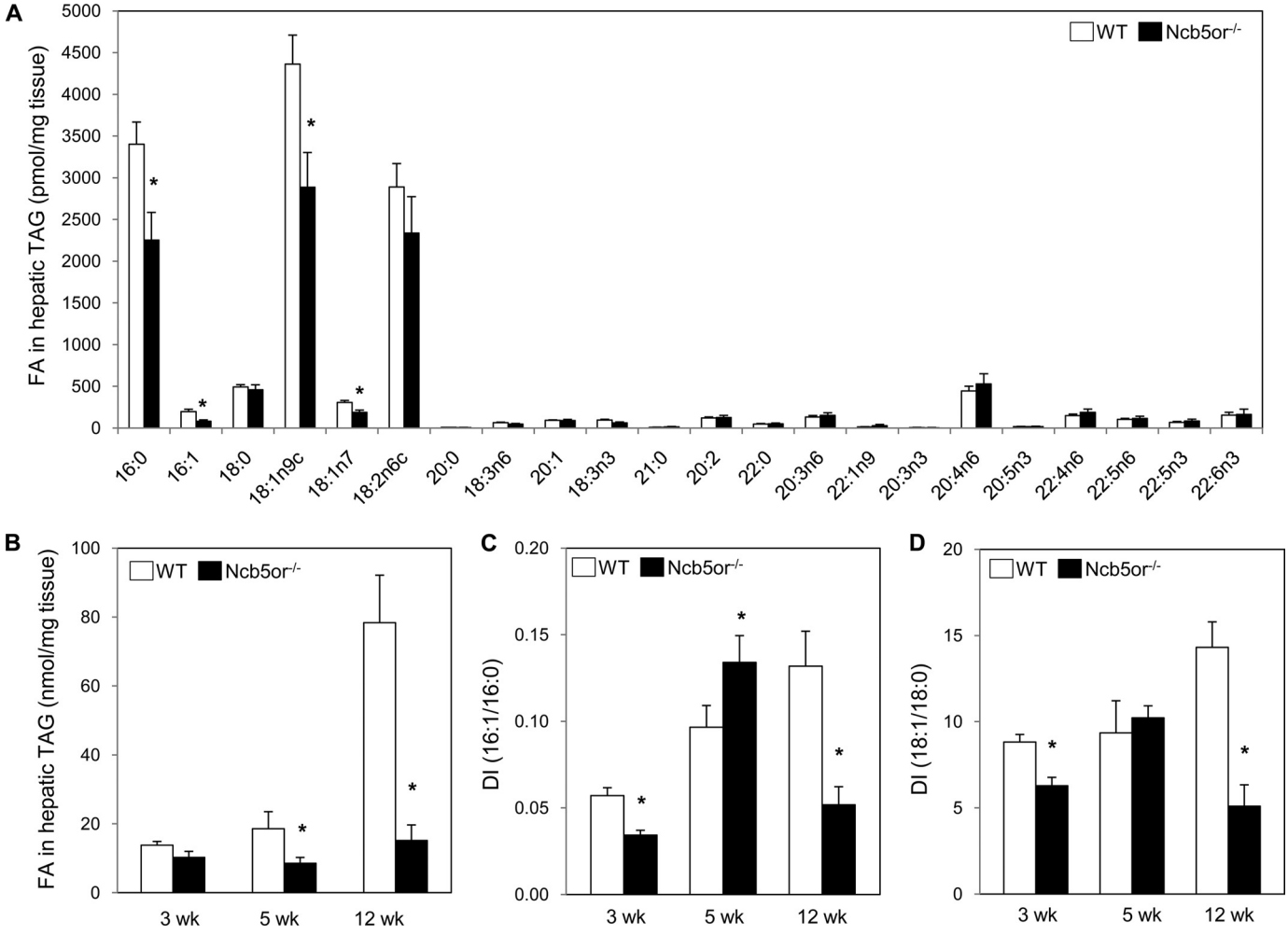

FIGURE 3. **Hepatic TAG content of chow-fed Ncb5or$^{-/-}$ and WT mice.** *A*, fatty acid (*FA*) composition of hepatic TAG from 3-week-old mice as determined by GC analysis is shown. Identical analyses were performed for hepatic TAG samples from 5- and 12-week-old mice. Values were used to calculate hepatic TAG level (*B*) and DI of 16:1/16:0 (*C*) and 18:1/18:0 (*D*) at all three ages. Results were obtained from 6–8 animals ($n = 6–8$) in each experimental group and are expressed as the mean ± S.E. *, $p < 0.05$. *White bar*, WT; *black bar*, Ncb5or$^{-/-}$.

Immunoblotting analyses confirmed increased expression of PGC-1α, SCD1, and eIF2α proteins and of the activated (phosphorylated) form of eIF2α in liver extract of Ncb5or$^{-/-}$ mice (Fig. 2, *B* and *C*). Consistent with increased expression of oxidative stress response genes, the fraction of glutathione in its oxidized form (GSSG) was also higher in Ncb5or$^{-/-}$ than in WT liver tissue (Fig. 2*D*) despite similar levels of total (reduced + oxidized) glutathione (Fig. 2*E*).

Temporal progression of gene expression was also measured in postnatal mouse livers of newborn, 2 and 3 weeks of age (Table 1). Expression of SCD1 and SCD2 (fatty acid desaturation), fatty acid synthase (synthesis), ACSL3 (activation/catab-

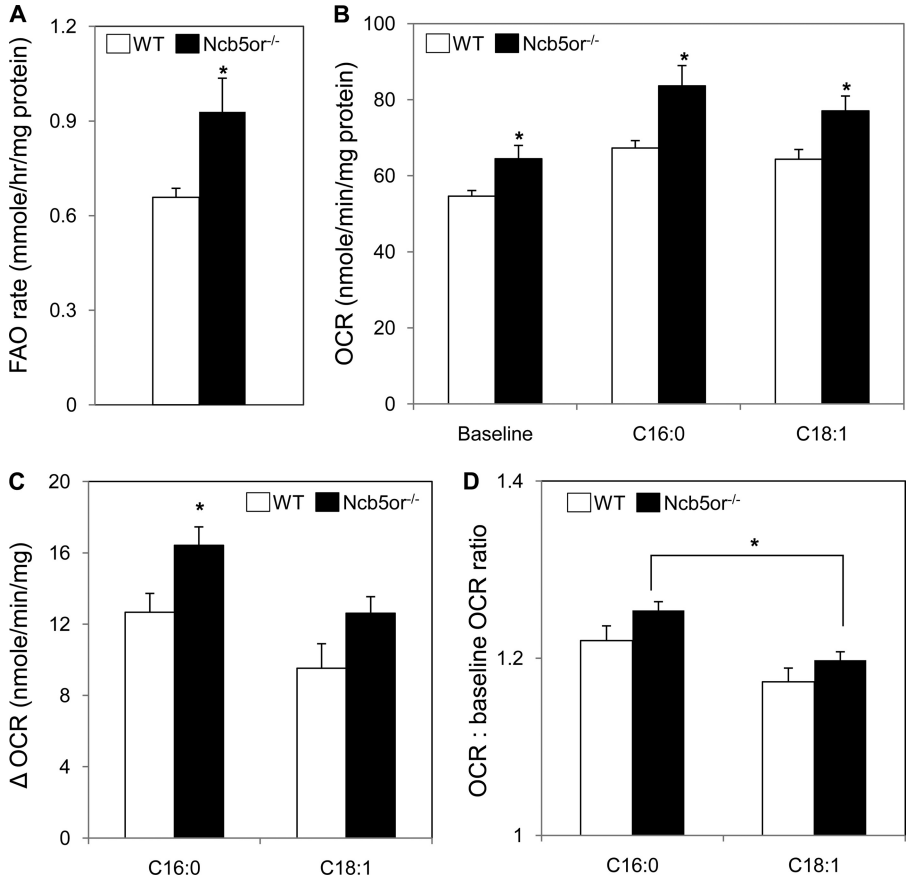

FIGURE 4. **Mitochondrial fatty acid oxidation in Ncb5or$^{-/-}$ and WT hepatocytes.** Hepatocytes were isolated from 4-week-old chow-fed WT and Ncb5or$^{-/-}$ mice and recovered overnight in medium containing 10% FBS. *A*, the rate of mitochondrial FAO was determined by incubating cells (37 °C, 2 h) with BSA-complexed palmitic acid (0.125 mM mixed with 0.8 μCi of [n9,10-^{3}H]palmitic acid) in the presence of 1 mM carnitine and measuring the oxidation product ([^{3}H]HO) in media. *B*, the same hepatocytes were subjected to extracellular flux analysis to measure OCR before (base line) and after the addition of 0.125 mM BSA-complexed palmitic acid (C16:0) or oleic acid (C18:1) in the presence of 1 mM carnitine. These values were used to calculate the increase in OCR (ΔOCR), shown in *C* and the relative change (OCR:base-line OCR ratio) shown in *D*. All results were obtained from four animal pairs ($n = 4$), standardized against total proteins of hepatocytes and expressed as the mean ± S.E. *, $p < 0.05$. *White bar*, WT; *black bar*, Ncb5or$^{-/-}$.

olism), and MT1 (oxidative stress response) genes was higher in Ncb5or$^{-/-}$ than in WT mice even for newborns. Within the first 3 weeks, transcript levels of genes in fatty acid uptake (Cluster of Differentiation 36 and lipoprotein lipase), mitochondrial biogenesis (PGC-1α), and oxidative stress (HMOX1 and GSTT3) also become higher in Ncb5or$^{-/-}$ than in WT liver. Hepatic SCD1 transcript levels peaked at 5 weeks and were 2-fold higher in Ncb5or$^{-/-}$ than WT. Hepatic PGC-1α transcript levels were highest in the neonatal period, then declined with age less rapidly in Ncb5or$^{-/-}$ than in WT and by 5 weeks were 1.8-fold higher in Ncb5or$^{-/-}$ than in WT livers. Increased expression of genes in *de novo* lipogenesis (SCD1, SCD2, fatty acid synthase), fatty acid activation/catabolism (ACSL3), and mitochondrial biogenesis (PGC-1α) are consistent with the futile fatty acid cycling in Ncb5or$^{-/-}$ liver, in which both fatty acid synthesis and catabolism are increased. No difference was observed between the two genotypes at 5 weeks of age in expression levels of other genes in lipogenesis, namely, DGAT2 (39), GPAT1 (40), and GPAT4 (41) (data not shown).

Reduced Hepatic TAG Contents in Ncb5or$^{-/-}$ Mice—We next isolated hepatic TAG chromatographically from mice of various ages and quantitated the TAG content of various fatty acid substituents. The three most abundant fatty acid substituents in hepatic TAG were palmitate (C16:0), oleate (C18:1n9c), and linoleate (C18:2n6c), and each was more abundant in WT than in Ncb5or$^{-/-}$ liver TAG at age 3 weeks (Fig. 3*A*), although the difference was significant only for C16:0 and C18:1. The total TAG content is reflected by the sum of the amounts of fatty acid substituents and was lower for Ncb5or$^{-/-}$ than for WT liver in all examined ages (Fig. 3*B*). This was significant both before and after the onset of diabetes, *i.e.* 5 and 12 weeks, respectively. In latter age, the hepatic TAG content in Ncb5or$^{-/-}$ mice was >5-fold lower than that of WT.

Palmitate (C16:0) is the principal product of fatty acid synthase in *de novo* lipogenesis and can be elongated to stearate (C18:0). These SFA can be converted to their corresponding MUFA, palmitoleate (C16:1), and oleate (C18:1), respectively, by SCD. The SCD activity is reflected by the MUFA:SFA ratio that we have designated as desaturation index (DI). Polyunsaturated fatty acids, such as linoleate, are essential; they or their precursors must be derived from dietary sources and cannot be synthesized *de novo*. The DI for 16-carbon (16:1/16:0) and 18-carbon (18:1/18:0) fatty acid substituents of hepatic TAG was significantly lower for Ncb5or$^{-/-}$ mice than for WT at age 3 weeks, and the difference was approximately 3-fold at 12

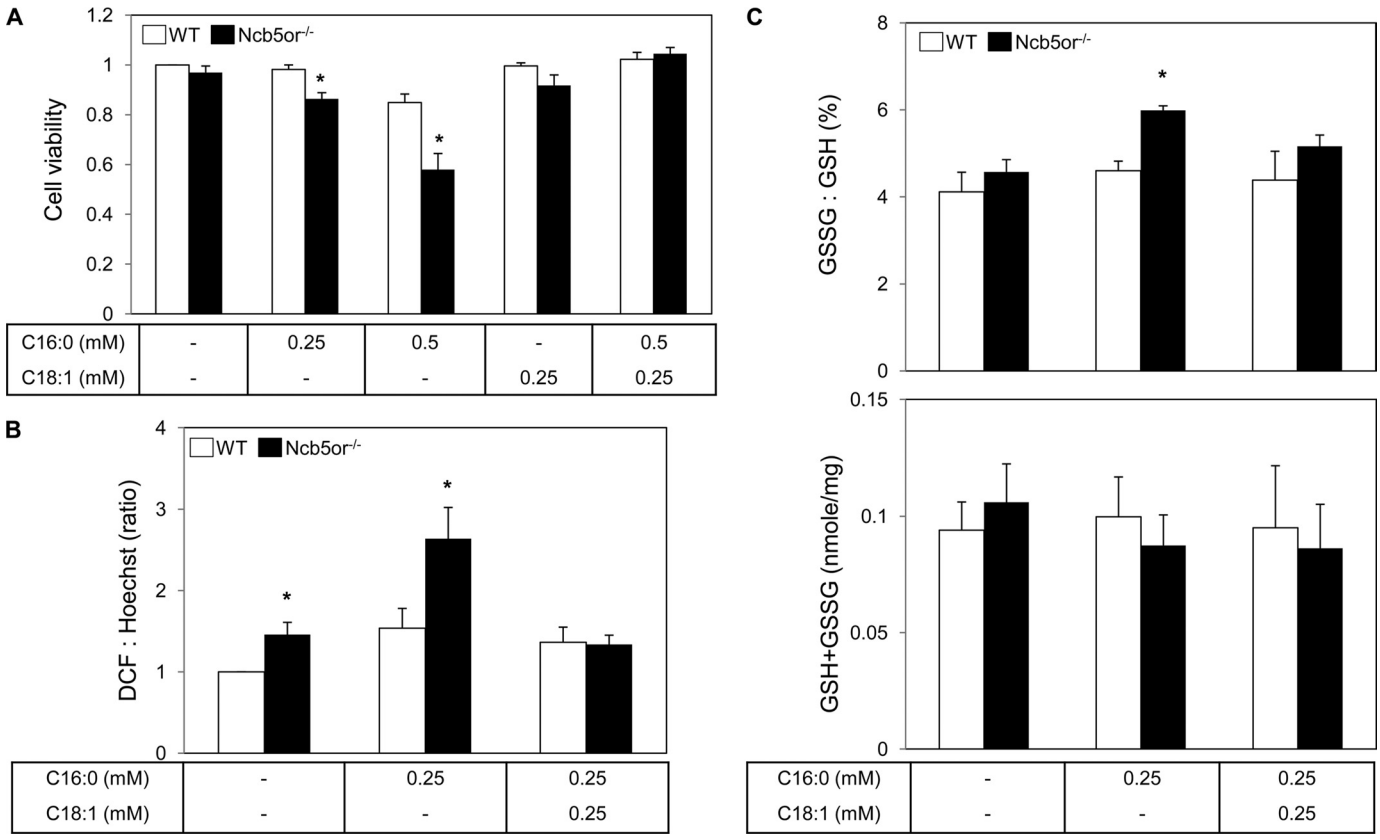

FIGURE 5. **Effects of incubation with palmitate and oleate on cell viability and oxidative stress marker expression in Ncb5or$^{-/-}$ and WT hepatocytes.** Hepatocytes were isolated as above and treated with BSA carrier (vehicle control, −) or BSA-complexed palmitic acid (C16:0) or oleic acid (C18:1) for 8 h. *A*, cell viability was assessed by measuring cellular ATP content. *B*, intracellular H_2O_2 content was assessed with 2′,7′-dichlorofluorescin diacetate, and relative intensity of fluorescence signals against nuclear DNA content (DCF:Hoechst ratio) was used in comparison. Images of DCF-stained hepatocytes are shown in supplemental Fig. 3. *C*, intracellular glutathione levels were measured and are displayed as the GSSG:GSH ratio (*top*) and GSH+GSSG (total glutathione content; *bottom panel*). All results were obtained from 4–6 animal pairs ($n = 4–6$) and are expressed as the mean ± S.E. *, $p < 0.05$. *White bar*, WT; *black bar*, Ncb5or$^{-/-}$.

weeks after the onset of diabetes (Fig. 3, *C* and *D*). The latter is concordant with a similar drop in DI values of liver lipids we previously observed in Ncb5or$^{-/-}$ mice whose diabetes was cured by transplantation of WT islets (6). There was a transient reversal of the DI of the hepatic TAG seen for WT and Ncb5or$^{-/-}$ mice at 5 weeks, possibly reflecting the up-regulation of hepatic SCD1 and SCD2 mRNA levels in Ncb5or$^{-/-}$ mice at that age (Fig. 2*A*).

Contributors to the reduced hepatic TAG content in Ncb5or$^{-/-}$ mice could include (*a*) decreased TAG synthesis, (*b*) increased secretion into circulation, or (*c*) enhanced oxidative catabolism of fatty acids that might be otherwise incorporated into TAG. The facts that hepatic expression levels of DGAT2, GAPT1, and GPAT4 genes are similar in Ncb5or$^{-/-}$ and WT mice (see above) and that rates of fatty acid incorporation into TAG are similar for isolated Ncb5or$^{-/-}$ and WT hepatocytes (see below) argue against defective TAG synthesis in Ncb5or$^{-/-}$ cells. The possibility that hepatic TAG secretion is increased in Ncb5or$^{-/-}$ mice is also unlikely because levels of plasma TAG and other lipids do not differ between Ncb5or$^{-/-}$ and WT mice (supplemental Table 1). To compare fatty acid catabolism in Ncb5or$^{-/-}$ and WT hepatocytes, we measured rates of FAO, as described below.

Higher Levels of Mitochondrial FAO and Cellular Respiration in Ncb5or$^{-/-}$ Hepatocytes—Isolated hepatocytes were incubated overnight in 10% FBS before exposure to exogenous fatty acids, and this protocol increased cell viability to 95% compared with 75% in previous studies in which FBS was not included in the recovery medium (4).

With palmitate as substrate, we observed a 30% higher rate of mitochondrial FAO with Ncb5or$^{-/-}$ compared with WT hepatocytes (Fig. 4*A*). Similar results were obtained with OCR measurements with Ncb5or$^{-/-}$ and WT hepatocytes in extracellular flux analyses upon adding buffer (base line) or BSA-complexed palmitate (C16:0) or oleate (C18:1) (Fig. 4, *B–D*). Ncb5or$^{-/-}$ hepatocytes exhibited higher OCR values than WT under all of these conditions (Fig. 4*B*). Although both palmitate and oleate induced a greater rise in OCR (ΔOCR) with Ncb5or$^{-/-}$ compared with WT hepatocytes (Fig. 4*C*), no difference between the genotypes was observed for the relative change (OCR:baseline OCR ratio) induced by palmitate or oleate (Fig. 4*D*). Palmitate induced significantly greater FAO than did oleate in Ncb5or$^{-/-}$ cells ($p = 0.012$), but no significant difference ($p = 0.16$) between palmitate and oleate was observed in the FAO responses of WT cells.

Ncb5or$^{-/-}$ and WT hepatocytes exhibited similar mitochondrial integrity when proton leak or non-mitochondrial oxygen consumption was tested with inhibitors for complex I, complex III, generation of proton gradient, and ATP synthesis (supplemental Fig. 2). These findings suggest that the increased mitochondrial FAO in Ncb5or$^{-/-}$ cells may be simply due to the increased mitochondrial density. The higher flux through

the mitochondrial electron transport chain in Ncb5or$^{-/-}$ cells is compatible with levels of oxidative stress, and this possibility was examined further in incubations with SFA or MUFA, as described below.

Increased Oxidative Stress for Ncb5or$^{-/-}$ Hepatocytes Challenged with SFA—Upon short term (8 h) incubation with exogenous fatty acids, loss of viability occurred more frequently with Ncb5or$^{-/-}$ than with WT hepatocytes exposed to palmitate (0.25–0.5 mM) but not oleate, and palmitate-induced cell death was prevented by co-incubation with oleate (Fig. 5*A*). Under our current conditions, palmitate treatment (0.25 mM for 8 h) induced greater cell death (15%) with Ncb5or$^{-/-}$ than with WT hepatocytes (3%). Similar results of cell viability were obtained by measuring cellular ATP content (above) and aminopeptidase or dipeptidyl aminopeptidase (data not shown). These findings are concordant with our previous reports on palmitate-induced cell death (4, 6).

We have previously observed that palmitate induces higher expression levels of the ER stress markers ATF3, ATF6, BiP, and CHOP in Ncb5or$^{-/-}$ compared with WT hepatocytes (4), but ER stress responses are less prominent in hepatocytes isolated and treated using the protocol in the current studies, which exhibit greater fractional viability than those in earlier studies (see above). No significant difference between genotypes in palmitate-induced ATF3 or ATF6 expression was observed, although Ncb5or$^{-/-}$ hepatocytes did exhibit palmitate-induced up-regulation of BiP and CHOP (not shown). Greater oxidation of the fluorescent marker DCF (Fig. 5*B* and supplemental Fig. 3) and a greater rise in the ratio of oxidized to reduced glutathione (Fig. 5*C*) occurred in Ncb5or$^{-/-}$ compared with WT hepatocytes, and these effects were prevented by co-incubation with oleate (Fig. 5, *B* and *C*, *top*). No significant changes in total (oxidized plus reduced) glutathione were observed under these conditions (Fig. 5*C*, *bottom*). DCF oxidation is generally taken to reflect its modification by reactive oxygen species, such as H_2O_2, and reduction of such species occurs at the expense of reduced glutathione (GSH) to yield its oxidized form (GSSG). The palmitate-induced cytotoxicity in Ncb5or$^{-/-}$ hepatocytes was also accompanied by increased induction of genes involved in mitochondrial biogenesis (PGC-1α) and oxidative stress responses (HMOX1, GCLC, MT1, and MT2), and these effects were prevented by co-incubation with oleate (Fig. 6).

Increased Accumulation of Palmitate in the Intracellular TAG and FFA Pools of Ncb5or$^{-/-}$ Hepatocytes upon Short Term Incubation—When hepatocytes were incubated with BSA-complexed palmitate under the conditions where differential cell loss and oxidative stress were observed with Ncb5or$^{-/-}$ cells (Figs. 5 and 6), a rise in TAG content occurred but did not differ between genotypes (Fig. 7*A*), suggesting an intact TAG synthesis in both Ncb5or$^{-/-}$ and WT cells. However, the DI (16:1/16:0) was significantly lower (by 1.6-fold) for the TAG pool (Fig. 7*A*) of Ncb5or$^{-/-}$ compared with WT hepatocytes. Oleate treatment alone abolished the difference in DI between genotypes, and co-incubation with palmitate and oleate (1:1) resulted in an even higher TAG content in Ncb5or$^{-/-}$ than WT hepatocytes (Fig. 7*A*). These observations suggested TAG remodeling in hepatocytes as a result of fatty

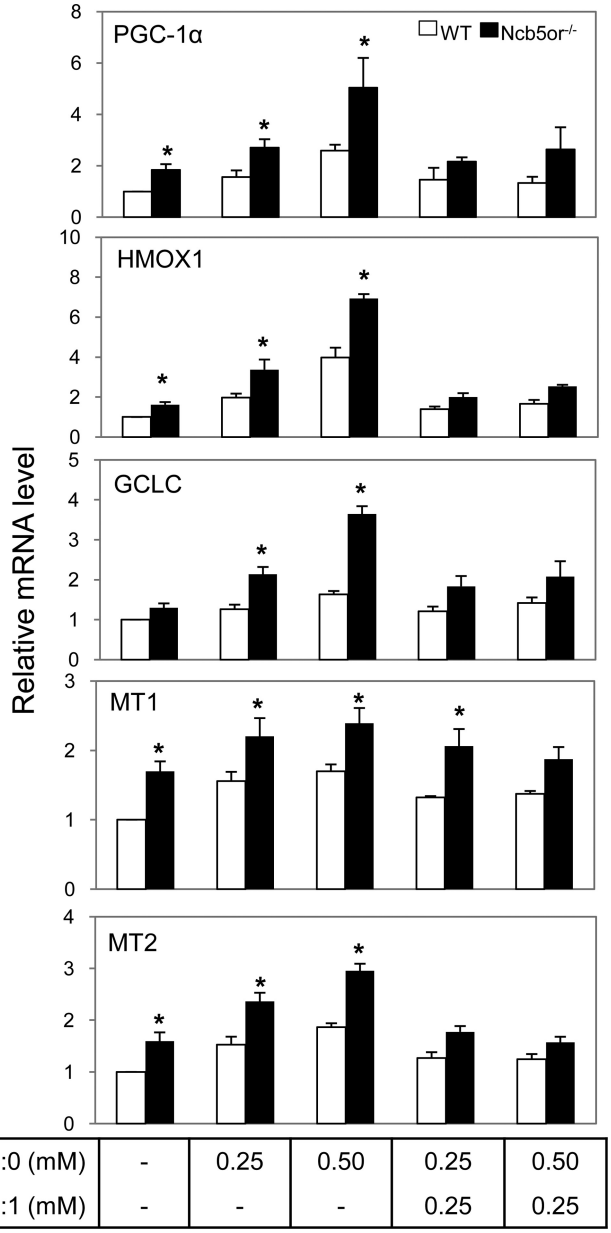

FIGURE 6. **Effects of incubation with palmitate and oleate on expression of genes involved in mitochondrial biogenesis and oxidative stress responses in Ncb5or$^{-/-}$ and WT hepatocytes.** Hepatocytes were isolated and treated with BSA-complexed palmitic or oleic acid or BSA carrier alone (see above). Total RNAs were collected and used for quantitative RT-PCR. Results were obtained from 4–6 animal pairs ($n = 4–6$) and are expressed as the mean ± S.E. *, $p < 0.05$. *White bar*, WT; *black bar*, Ncb5or$^{-/-}$.

acid treatments, a process also revealed by GC-MS analyses of total cellular lipids.[5] No significant difference was found between genotypes in GPAT1, GPAT4, DGAT2, SCD1, and SCD2 expression in palmitate treatment (supplemental Fig. 4); therefore, an overabundance of fatty acid substrates rather than the altered levels of key enzymes in TAG synthesis and fatty acid desaturation is likely responsible for a similar TAG content but a lower DI (16:1/16:0) value in Ncb5or$^{-/-}$ than WT cells.

Consistently, a significantly higher FFA content was observed in Ncb5or$^{-/-}$ compared with WT hepatocytes under

[5] H. Zhu, F. Hsu, and J. Turk, unpublished results.

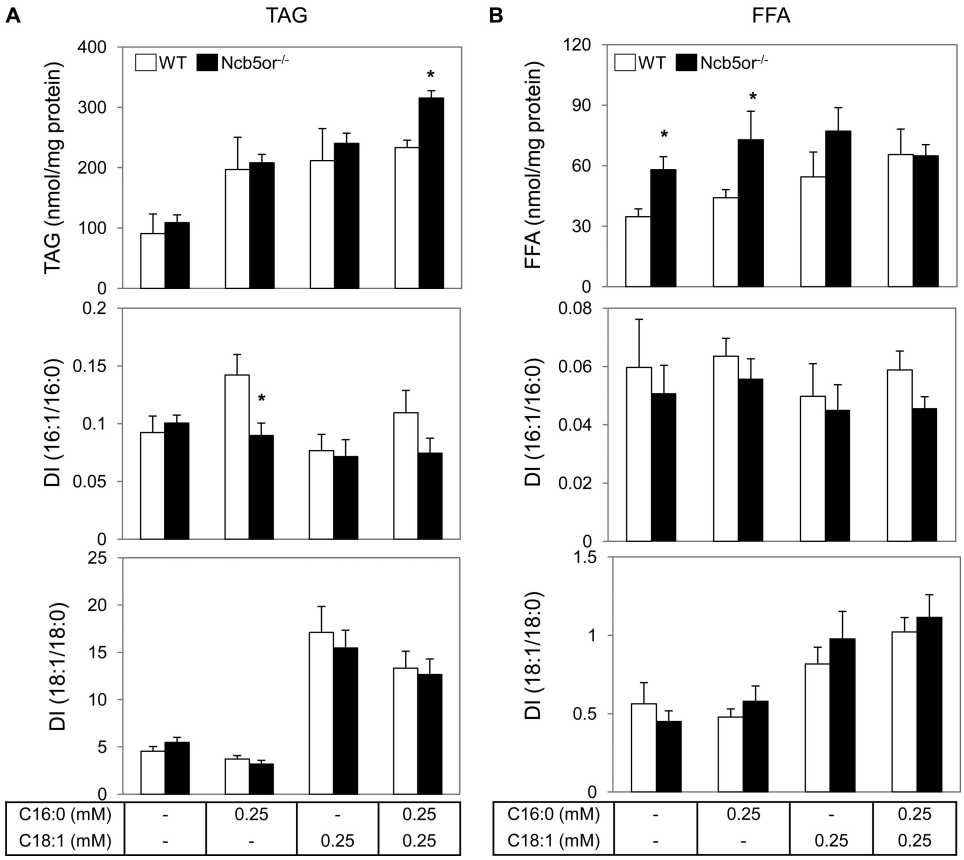

FIGURE 7. **Effects of incubation with palmitate and oleate on Ncb5or$^{-/-}$ and WT hepatocyte TAG and FFA pools.** Hepatocytes were isolated and treated with BSA-complexed palmitic or oleic acid or BSA carrier alone (see above). Intracellular FFA and TAG were prepared and analyzed for determination of lipid profiles by GC-MS. The total content, desaturation index of C16:1/C16:0 and C18:1/C18:0, was determined for TAG (*A*) and FFA (*B*). Results were obtained from 4–6 animal pairs ($n = 4–6$) for TAG and FFA profiling and are expressed as the mean ± S.E. *, $p < 0.05$. *White bar*, WT; *black bar*, Ncb5or$^{-/-}$. *FA*, fatty acid.

basal conditions and upon incubation with palmitate but not oleate or the palmitate/oleate mixture (Fig. 7*B*). The two genotypes had similar DI values under all four conditions. Greater accumulation of free palmitate, thus, correlates with a higher level of oxidative stress in Ncb5or$^{-/-}$ compared with WT hepatocytes under basal conditions or upon incubation with exogenous palmitate. Incubation with oleate or with both palmitate and oleate appears to channel fatty acids into TAG synthesis in Ncb5or$^{-/-}$ cells, which abolishes the difference between Ncb5or$^{-/-}$ and WT hepatocytes in intracellular fatty acid accumulation (Fig. 7*B*) and thereby reduces expression of oxidative stress markers (Fig. 5*B*). Notably, increased accumulation of intracellular palmitate in Ncb5or$^{-/-}$ cells resulted in no significant change in total ceramide content or the d18:1/16:0 ceramide species (supplemental Fig. 5).

High Fat Feeding Stimulated Lipogenesis, Fatty Acid Catabolism, and Oxidase Stress Response in Ncb5or$^{-/-}$ Livers—To examine genotype effects on responses to dietary interventions in whole animals *in vivo*, Ncb5or$^{-/-}$ and WT mice were fed a high fat diet rich in both SFAs and MUFAs for 10 days starting at age 3 weeks, and the lipid contents of their liver tissues were then examined. As noted above, both body weights and hepatic TAG content were found to be lower in chow-fed Ncb5or$^{-/-}$ than WT mice of age 3–5 weeks (Fig. 3*B*). After 10 days of consuming the high fat diet, Ncb5or$^{-/-}$ mice maintained lower body weights (not shown) and higher hepatic FFA content than did WT (Fig. 8*A*). Hepatic TAG content, however, became equivalent between genotypes (Fig. 8*B*), and the DI values of 16:1/16:0 and 18:1/18:0 were higher in Ncb5or$^{-/-}$ than WT mice (Fig. 8, *C* and *D*).

Consistently, the high fat feeding induced a greater fold increase of hepatic transcript levels in Ncb5or$^{-/-}$ mice (compared with WT) than chow-fed mice for genes involved in fatty acid biosynthesis and desaturation (fatty acid synthase (6.7-fold), SCD1 (9.2-fold), Cyb5A (1.2-fold), FADS2 (5.5-fold)), fatty acid/lipid uptake (lipoprotein lipase (4.5-fold) and Cluster of Differentiation 36 (2.3-fold)), glycerolipid/TAG synthesis (GPAT1, GPAT4, and DGAT2 (2.3–2.9-fold)), and fatty acid activation (ACSL1, ACSL4, and ACSL5 (1.3–2.7-fold)) (42–44) and upstream regulators (peroxisome proliferator-activated receptor α (PPARα) and PPARδ (2.5–3.3-fold)) (33, 45, 46), mitochondrial biogenesis (PGC-1α (2.9-fold)), and oxidative stress response (HMOX-1 (3.4-fold) and GSTT3 (4.9-fold)) (Table 2). Up-regulation of SCD2, MT1, MT2, and ACSL3 in Ncb5or$^{-/-}$ mice fed the high fat diet were similar to that of chow-fed mice.

Despite increased fatty acid catabolism, hepatic TAG content in Ncb5or$^{-/-}$ mice was restored after 10 days of consuming the high fat diet. This suggests that a prolonged intake of this high fat diet may fully restore adiposity in Ncb5or$^{-/-}$ mice,

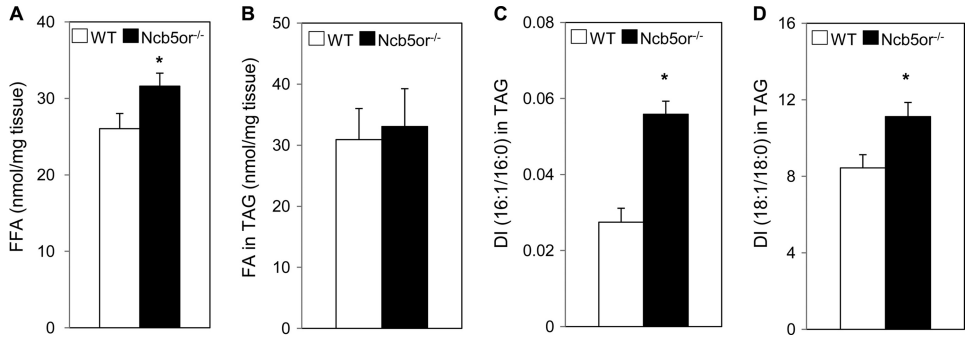

FIGURE 8. **Effects of a 10-day high fat diet feeding on hepatic lipid content of Ncb5or$^{-/-}$ and WT mice.** After 10 days on high fat diet, the amount of hepatic lipids as FFA (*A*) and TAG (*B*) from 4.5-week-old WT ($n = 9$) and Ncb5or$^{-/-}$ ($n = 6$) mice was determined by colorimetric assay and GC-MS, respectively. Desaturation indices of hepatic TAG are plotted for 16:1/16:0 (*C*) and 18:1/18:0 (*D*). Results are expressed as the mean ± S.E. *, $p < 0.05$. *White bar*, WT; *black bar*, Ncb5or$^{-/-}$.

TABLE 2

Transcript levels of genes involved in lipid metabolism, mitochondrial biogenesis, and oxidative stress response in 4.5-week-old Ncb5or$^{-/-}$ and WT mouse livers after 10 days of high fat feeding

All values are the mean ± S.E. ($n = 6$) and relative to 18S ($\times 10^6$). FAS, fatty acid sythase; PPAR, peroxisome proliferator-activated receptor; LPL, lipoprotein lipase.

	WT	Ncb5or$^{-/-}$	Fold increase in Ncb5or$^{-/-}$
SCD1	103 ± 12	947 ± 158[a]	9.2
SCD2	1.23 ± 0.11	1.75 ± 0.25	1.4
FADS2	26.4 ± 4.3	144 ± 27[a]	5.5
GPAT1	19.6 ± 1.8	45.2 ± 7.0[a]	2.3
GPAT4	5.69 ± 1.04	16.3 ± 2.2[a]	2.9
DGAT2	52.5 ± 4.4	121 ± 17[a]	2.3
Cyb5A	353 ± 9	432 ± 18[a]	1.2
FAS	3.19 ± 0.41	21.4 ± 5.4[a]	6.7
PGC-1α	3.56 ± 0.64	10.4 ± 1.3[a]	2.9
PPARα	11.2 ± 1.2	28.4 ± 2.8[a]	2.5
PPARδ	0.29 ± 0.05	0.97 ± 0.14[a]	3.3
ACSL1	31.2 ± 3.1	41.9 ± 1.7[b]	1.3
ACSL3	0.83 ± 0.13	2.03 ± 0.29[a]	2.4
ACSL4	4.35 ± 0.51	6.45 ± 0.71[b]	1.5
ACSL5	5.72 ± 0.42	15.2 ± 1.7[a]	2.7
CD36	6.11 ± 0.52	14.2 ± 2.3[a]	2.3
LPL	10.2 ± 0.6	45.6 ± 6.7[a]	4.5
MT1	37.8 ± 9.1	354 ± 70[a]	9.4
MT2	7.40 ± 2.04	89.1 ± 14.7[a]	12
HMOX1	3.12 ± 0.39	10.6 ± 1.4[a]	3.4
GSTT3	1.96 ± 0.38	9.50 ± 2.23[a]	4.9

[a] $p < 0.005$.
[b] $p < 0.05$.

which has been confirmed in a separate study.[6] Similar to chow-fed mice, the high fat fed Ncb5or$^{-/-}$ mice had a higher hepatic FFA content than did WT, correlating to increased expression of oxidative stress genes in Ncb5or$^{-/-}$ liver. Nonetheless, there was no detectable histological hepatic inflammation (supplemental Fig. 6) and no hepatocyte apoptosis by TUNEL staining in Ncb5or$^{-/-}$ mice after consuming a high fat diet for 10 days (not shown).

Lower SCD Specific Activity in Ncb5or$^{-/-}$ Liver Microsomes—There is a notable discrepancy in the magnitude of up-regulated SCD1 gene expression (transcripts) induced by the high fat diet (9-fold, Table 2) compared with the less than 2-fold increase in the DI of 16:1/16:0 and 18:1/18:0 (Fig. 8). To investigate further, we isolated microsomes from liver tissue of Ncb5or$^{-/-}$ and WT mice and determined their SCD activities directly by measuring conversion of [^{14}C]stearoyl-CoA to [^{14}C]oleoyl-CoA. With livers from mice fed either chow or a high fat diet, absolute SCD activity was ~2-fold higher for Ncb5or$^{-/-}$ than for WT microsomes (Fig. 9, *A* and *C*), and this was statistically significant for mice fed the high fat diet (Fig. 9*C*). In contrast, the SCD specific activity, *i.e.* activity *versus* SCD1 transcript level, was significantly lower for Ncb5or$^{-/-}$ than for WT microsomes, and this was much more drastic for mice fed a high fat diet (Ncb5or$^{-/-}$/WT < 0.2) than for those fed chow (Ncb5or$^{-/-}$/WT ~0.74) (Fig. 9, *B* and *D*). To test whether the lower SCD specific activity (SCD:SCD1 mRNA ratio) in Ncb5or$^{-/-}$ hepatocytes reflects a lower amount of the SCD1 protein per given transcripts, the level of SCD1 protein was examined by denaturing protein gel electrophoresis (SDS-PAGE) and immunoblotting with an SCD1 antibody. It was found that the relative intensity of the band for immunoreactive SCD1 divided by that for β-actin was about 8-fold higher for Ncb5or$^{-/-}$ than for WT hepatic microsomes (Fig. 9*E*), which is concordant with the 9-fold higher SCD1 transcript level in Ncb5or$^{-/-}$ hepatocytes. These findings indicate that SCD1 proteins in Ncb5or$^{-/-}$ hepatic microsomes have lower specific activities than those in WT microsomes. This defect is exaggerated upon consumption of a high fat diet that increases fatty acid catabolism and oxidative stress in Ncb5or$^{-/-}$ hepatocytes while imposing a greater demand for lipogenesis.

DISCUSSION

Our current study characterizes hepatic lipid metabolic abnormalities and their progression with age in Ncb5or-null mice. Abnormalities include increased uptake, synthesis, accumulation, and oxidation of fatty acids, dysregulated fatty acid desaturation, and reduced TAG deposition (Fig. 10). Defects in early neonatal development lead to increased mitochondrial biogenesis, fatty acid catabolism, and oxidative stress, and these phenotypic abnormalities are exacerbated by exposure to excess SFA and attenuated by MUFA. These findings are similar to those reported for SCD1-deficient cells (47), suggesting that inactivation of Ncb5or or SCD1 produces a common biochemical defect.

It is notable that hepatic TAG stores in Ncb5or$^{-/-}$ mice exhibited fatty acid desaturation indices that were significantly lower than those of WT mice as early as age 3 weeks when fed with chow. This was also the case for Ncb5or$^{-/-}$ hepatocytes incubated with palmitate. Such results would be expected in the setting of dysregulated SCD reaction because it is tightly cou-

[6] M. Xu, W. Wang, and H. Zhu, unpublished results.

pled to TAG synthesis (48) and likely mediated by the co-localization of SCD1 with DGAT2 (49). TAG synthesis appears to remain intact in Ncb5or$^{-/-}$ cells because they can restore intracellular TAG content to WT levels upon acute fatty acid supplementation. Restoration of hepatic TAG content also occurs in Ncb5or-null mice on a high fat diet as a result of increased expression of SCD1, DGAT2, and other lipogenic genes. Global SCD1-null mice have reduced TAG content due to their impaired ability to generate MUFA (48). Recent studies show that hepatic SCD1$^{-/-}$ mice are resistant to obesity induced by a high carbohydrate diet (50) but not to obesity induced by a high fat diet, suggesting that another SCD isoform(s) may be involved in the desaturation of exogenous SFA from dietary sources. Notably, SCD1 deficiency exacerbates diabetes in leptin-deficient obese mice, although SCD1$^{-/-}$ mice do not develop diabetes *per se* (51).

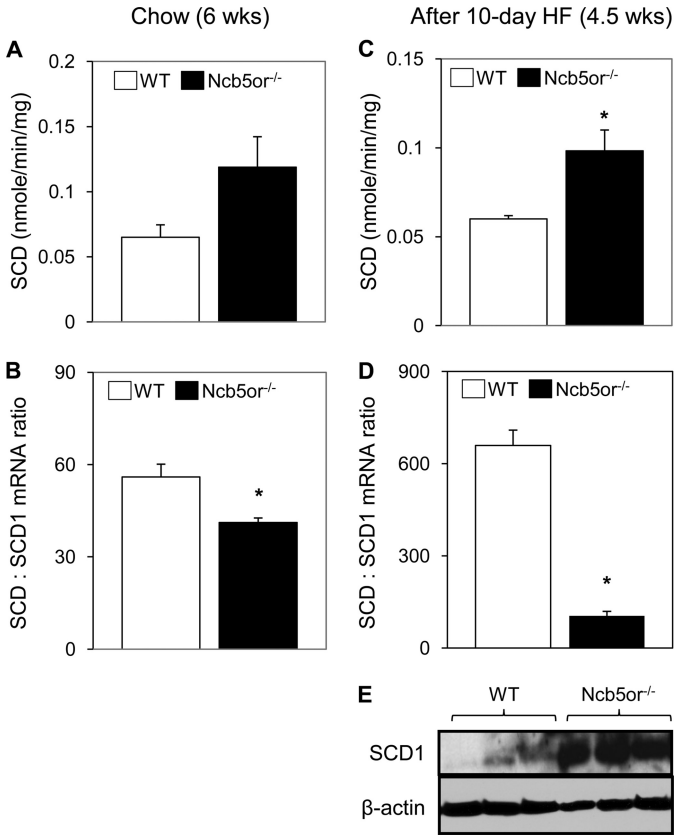

FIGURE 9. **SCD activity and levels of SCD1 transcripts and SCD immunoreactive protein in hepatic microsomes from Ncb5or$^{-/-}$ and WT mice.** SCD activities were measured for WT and Ncb5or$^{-/-}$ liver microsomes of 6-week-old chow-fed (*A*) and 4.5-week-old mice after 10 days of high fat feeding (*C*). Absolute activity (nmol/min/mg) was divided by SCD1 mRNA (calculated as those in Tables 1 and 2) to calculate specific activity "SCD:SCD1 mRNA ratio," as plotted in *B* and *D*, respectively. Results were obtained from 3 ($n = 3$) chow-fed or 6 ($n = 6$) high fat animal pairs and are expressed as the mean ± S.E. *E*, immunoblot analysis showed a >8-fold more SCD1 proteins (against β-actin loading control) in the liver lysate ($n = 3$ each) of high fat-fed Ncb5or$^{-/-}$ than WT mice. *White bar*, WT; *black bar*, Ncb5or$^{-/-}$. *, $p < 0.05$.

Exogenous palmitate mainly distributes among intracellular TAG and FFA pools upon entry into cells (52). Increased SFA accumulation within intracellular fatty acid pools appears to be a central event in the network of responses in Ncb5or-null cells, which ultimately results in oxidative stress (current study) and ER stress (4), similar to observation reported by others (53). Our current study reveals increased activation of eIF2α in Ncb5or$^{-/-}$ livers, which is likely involved in both oxidative stress and ER stress response pathways as previously shown (54). SFAs are known to induce expression of PGC-1β and PGC-1α (55), both of which can increase the activities of oxidative metabolic pathways, mitochondrial expansion, and mitochondrial FAO. Indeed, increases in PGC-1α expression, fatty acid catabolism, cellular oxidative stress, and expression of oxidative stress response genes were observed in SFA-treated Ncb5or-null hepatocytes. The fact that Ncb5or$^{-/-}$ and WT hepatocytes did not differ in TAG synthesis upon incubation with palmitate suggests that SFA accumulation rather than differential TAG channeling (56) is responsible for the increased susceptibility of Ncb5or$^{-/-}$ cells to cytotoxic effects of palmitate.

Higher levels of intracellular FFA accumulation and oxidative stress are coincidently observed in livers of Ncb5or$^{-/-}$ mice fed a high fat diet. Our *in vivo* and *in vitro* experiments differ in the nature of the biochemical species in which the fatty acids are provided (TAG *versus* FFA), in the relative amounts of fatty acid equivalents provided (low *versus* high), and in the intervals over which the fatty acid equivalents were provided (days *versus* hours). Circulating fatty acids in mice are mainly esterified in TAG, so FFA concentrations are low. Fatty acid metabolism in white adipose tissues and skeletal muscle,

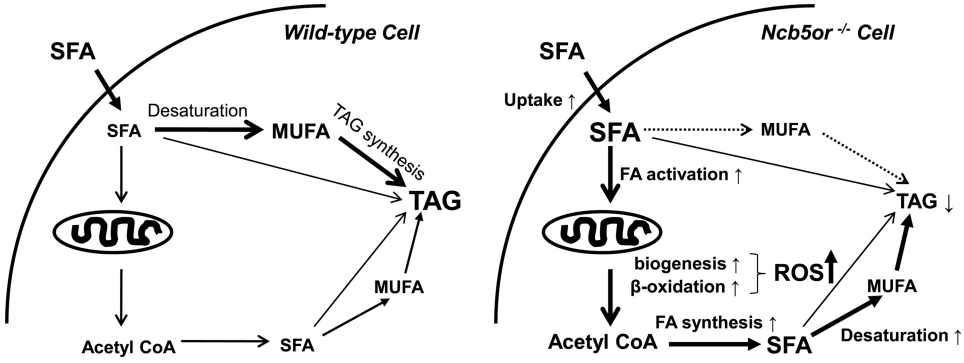

FIGURE 10. **Working hypothesis of Ncb5or deficiency decreases SCD efficiency and increases fatty acid catabolism and oxidative stress.** *Left*, after an update into wild-type cells, exogenous SFAs are converted to MUFAs and preferably incorporated into TAG (anabolism) rather than oxidized to acetyl-CoA in mitochondria (catabolism). *Right*, Ncb5or$^{-/-}$ hepatocytes have a lower capacity to convert exogenous SFAs to MUFAs for TAG synthesis. The higher accumulation of intracellular FFA induces higher levels of fatty acid oxidation, mitochondrial proliferation, and oxidative stress. Exposure to excess SFA induces more oxidative stress and leads to cell death, whereas co-incubation of MUFAs attenuates cytotoxicity by channeling fatty acids into the TAG pool.

among other tissues, is expected to weaken the rescue effect of MUFA in liver of KO mice. Thus, the attenuation of fatty acid-induced oxidative stress by channeling fatty acids into TAG synthesis and away from oxidative metabolism occurs more slowly in the liver of KO mice fed a high fat diet *in vivo* than is the case for KO hepatocytes incubated with FFA *in vitro*. Despite increased TAG synthesis, livers of Ncb5or-null mice fed a high fat diet maintain high levels of intracellular fatty acid accumulation and oxidative stress. Proinflammatory cytokine has been implicated in SFA-induced hepatic cytotoxicity (57). Our current study, however, reveals no histological detectable inflammation in livers of Ncb5or$^{-/-}$ mice despite minor increase in expression of proinflammatory cytokine genes.[6] Their role in Ncb5or-null liver tissue and hepatocytes is the focus of ongoing investigation. The lack of difference in ceramide profile between Ncb5or$^{-/-}$ and WT cells suggests a ceramide-independent pathway of cell loss under palmitate challenge, which has been reported by others (58, 59).

Our observations raise important questions about the mechanism underlying SCD dysregulation in Ncb5or$^{-/-}$ cells. Among several possibilities, one is that SCD1 requires a redox partner(s) as the electron donor(s) that is present in WT cells but under-represented in Ncb5or$^{-/-}$ hepatocytes. Unlike Δ5 and Δ6 desaturases from mammals (60, 61) and Δ9 desaturase from bakers' yeast (62, 63), SCDs in mammals have no intrinsic electron donor domain and, therefore, require a redox partner. Although Cyb5A and Cyb5R3 fulfill such a role *in vitro*, they are not obligate or exclusive redox partners for SCD because SCD index is mildly reduced in hepatic lipids of Cyb5A-null mice (10), in contrast to a greater reduction in Ncb5or-null (6) and in SCD-null mice (48), and no significant change is found in lipids of brain, kidney, or liver from patients with a methemoglobinemia-carrying mutation(s) in the Cyb5R3 or Cyb5A genes (64, 65). It is also possible that Ncb5or cooperates with other redox partners and that Ncb5or deficiency indirectly impacts SCD functionality. Iron has been shown to be an essential cofactor that is required for SCD catalytic activity (66–70). Additional studies involving genetic models, dietary interventions, and biochemical and molecular analyses are under way to examine these possibilities. Identification of Ncb5or partners *in vivo* is also desired for future studies.

Acknowledgments—We thank H. Franklin Bunn at Brigham and Women's Hospital for generous support and critical reading of the manuscript and the journal reviewers for constructive comments. We acknowledge colleagues at University of Kansas Medical Center for advice and assistance: Grace Guo (high fat dietary treatment), Bryan Copple (hepatocyte isolation), Hartmut Jaeschke (glutathione measurements), Barbara Fegley (electron microscopy), Bin Deng (lipid analysis), and Han-Hung Huang and Lisa Stehno-Bittel (confocal microscopy).

REFERENCES

1. Zhu, H., Qiu, H., Yoon, H. W., Huang, S., and Bunn, H. F. (1999) *Proc. Natl. Acad. Sci. U.S.A.* **96,** 14742–14747
2. Garcia-Ranea, J. A., Mirey, G., Camonis, J., and Valencia, A. (2002) *FEBS Lett.* **529,** 162–167
3. Xie, J., Zhu, H., Larade, K., Ladoux, A., Seguritan, A., Chu, M., Ito, S., Bronson, R. T., Leiter, E. H., Zhang, C. Y., Rosen, E. D., and Bunn, H. F. (2004) *Proc. Natl. Acad. Sci. U.S.A.* **101,** 10750–10755
4. Zhang, Y., Larade, K., Jiang, Z. G., Ito, S., Wang, W., Zhu, H., and Bunn, H. F. (2010) *J. Lipid Res.* **51,** 53–62
5. Larade, K., Jiang, Z. G., Dejam, A., Zhu, H., and Bunn, H. F. (2007) *Biochem. J.* **404,** 467–476
6. Larade, K., Jiang, Z., Zhang, Y., Wang, W., Bonner-Weir, S., Zhu, H., and Bunn, H. F. (2008) *J. Biol. Chem.* **283,** 29285–29291
7. Miyazaki, M., Kim, Y. C., Gray-Keller, M. P., Attie, A. D., and Ntambi, J. M. (2000) *J. Biol. Chem.* **275,** 30132–30138
8. Strittmatter, P., Spatz, L., Corcoran, D., Rogers, M. J., Setlow, B., and Redline, R. (1974) *Proc. Natl. Acad. Sci. U.S.A.* **71,** 4565–4569
9. Finn, R. D., McLaughlin, L. A., Ronseaux, S., Rosewell, I., Houston, J. B., Henderson, C. J., and Wolf, C. R. (2008) *J. Biol. Chem.* **283,** 31385–31393
10. Finn, R. D., McLaughlin, L. A., Hughes, C., Song, C., Henderson, C. J., and Roland Wolf, C. (2010) *Transgenic Res.* [Epub ahead of print]
11. Zhu, H., Larade, K., Jackson, T. A., Xie, J., Ladoux, A., Acker, H., Berchner-Pfannschmidt, U., Fandrey, J., Cross, A. R., Lukat-Rodgers, G. S., Rodgers, K. R., and Bunn, H. F. (2004) *J. Biol. Chem.* **279,** 30316–30325
12. Gardner, A. M., Cook, M. R., and Gardner, P. R. (2010) *J. Biol. Chem.* **285,** 23850–23857
13. Deng, B., Parthasarathy, S., Wang, W., Gibney, B. R., Battaile, K. P., Lovell, S., Benson, D. R., and Zhu, H. (2010) *J. Biol. Chem.* **285,** 30181–30191
14. Andersen, G., Wegner, L., Rose, C. S., Xie, J., Zhu, H., Larade, K., Johansen, A., Ek, J., Lauenborg, J., Drivsholm, T., Borch-Johnsen, K., Damm, P., Hansen, T., Bunn, H. F., and Pedersen, O. (2004) *Diabetes* **53,** 2992–2997
15. Sjöblom, T., Jones, S., Wood, L. D., Parsons, D. W., Lin, J., Barber, T. D., Mandelker, D., Leary, R. J., Ptak, J., Silliman, N., Szabo, S., Buckhaults, P., Farrell, C., Meeh, P., Markowitz, S. D., Willis, J., Dawson, D., Willson, J. K., Gazdar, A. F., Hartigan, J., Wu, L., Liu, C., Parmigiani, G., Park, B. H., Bachman, K. E., Papadopoulos, N., Vogelstein, B., Kinzler, K. W., and Velculescu, V. E. (2006) *Science* **314,** 268–274
16. Lagouge, M., Argmann, C., Gerhart-Hines, Z., Meziane, H., Lerin, C., Daussin, F., Messadeq, N., Milne, J., Lambert, P., Elliott, P., Geny, B., Laakso, M., Puigserver, P., and Auwerx, J. (2006) *Cell* **127,** 1109–1122
17. Folch, J., Lees, M., and Sloane, Stanley, G. H. (1957) *J. Biol. Chem.* **226,** 497–509
18. Morrison, W. R., and Smith, L. M. (1964) *J. Lipid Res.* **5,** 600–608
19. Kim, N. D., Moon, J. O., Slitt, A. L., and Copple, B. L. (2006) *Toxicol. Sci.* **90,** 586–595
20. Wolins, N. E., Skinner, J. R., Schoenfish, M. J., Tzekov, A., Bensch, K. G., and Bickel, P. E. (2003) *J. Biol. Chem.* **278,** 37713–37721
21. Bligh, E. G., and Dyer, W. J. (1959) *Can. J. Biochem. Physiol* **37,** 911–917
22. Hsu, F. F., and Turk, J. (2002) *J. Am. Soc. Mass Spectrom.* **13,** 558–570
23. Djouadi, F., Bonnefont, J. P., Munnich, A., and Bastin, J. (2003) *Mol. Genet. Metab.* **78,** 112–118
24. Zhang, L., Yu, C., Vasquez, F. E., Galeva, N., Onyango, I., Swerdlow, R. H., and Dobrowsky, R. T. (2010) *J. Proteome Res.* **9,** 458–471
25. Jaeschke, H., and Mitchell, J. R. (1990) *Methods Enzymol.* **186,** 752–759
26. Miyazaki, M., Kim, H. J., Man, W. C., and Ntambi, J. M. (2001) *J. Biol. Chem.* **276,** 39455–39461
27. Wu, Z., Puigserver, P., Andersson, U., Zhang, C., Adelmant, G., Mootha, V., Troy, A., Cinti, S., Lowell, B., Scarpulla, R. C., and Spiegelman, B. M. (1999) *Cell* **98,** 115–124
28. Ntambi, J. M., Buhrow, S. A., Kaestner, K. H., Christy, R. J., Sibley, E., Kelly, T. J., Jr., and Lane, M. D. (1988) *J. Biol. Chem.* **263,** 17291–17300
29. Kaestner, K. H., Ntambi, J. M., Kelly, T. J., Jr., and Lane, M. D. (1989) *J. Biol. Chem.* **264,** 14755–14761
30. Paulauskis, J. D., and Sul, H. S. (1988) *J. Biol. Chem.* **263,** 7049–7054
31. Kirchgessner, T. G., Svenson, K. L., Lusis, A. J., and Schotz, M. C. (1987) *J. Biol. Chem.* **262,** 8463–8466
32. Febbraio, M., Abumrad, N. A., Hajjar, D. P., Sharma, K., Cheng, W., Pearce, S. F., and Silverstein, R. L. (1999) *J. Biol. Chem.* **274,** 19055–19062
33. Cao, A., Li, H., Zhou, Y., Wu, M., and Liu, J. (2010) *J. Biol. Chem.* **285,** 16664–16674
34. Coggan, M., Flanagan, J. U., Parker, M. W., Vichai, V., Pearson, W. R., and Board, P. G. (2002) *Biochem. J.* **366,** 323–332
35. Huang, I. Y., and Yoshida, A. (1977) *J. Biol. Chem.* **252,** 8217–8221

36. Huang, I. Y., Kimura, M., Hata, A., Tsunoo, H., and Yoshida, A. (1981) *J. Biochem.* **89,** 1839–1845
37. Kageyama, H., Hiwasa, T., Tokunaga, K., and Sakiyama, S. (1988) *Cancer Res.* **48,** 4795–4798
38. Scheuner, D., Song, B., McEwen, E., Liu, C., Laybutt, R., Gillespie, P., Saunders, T., Bonner-Weir, S., and Kaufman, R. J. (2001) *Mol Cell* **7,** 1165–1176
39. Cases, S., Stone, S. J., Zhou, P., Yen, E., Tow, B., Lardizabal, K. D., Voelker, T., and Farese, R. V., Jr. (2001) *J. Biol. Chem.* **276,** 38870–38876
40. Hammond, L. E., Neschen, S., Romanelli, A. J., Cline, G. W., Ilkayeva, O. R., Shulman, G. I., Muoio, D. M., and Coleman, R. A. (2005) *J. Biol. Chem.* **280,** 25629–25636
41. Nagle, C. A., Vergnes, L., Dejong, H., Wang, S., Lewin, T. M., Reue, K., and Coleman, R. A. (2008) *J. Lipid Res.* **49,** 823–831
42. Mashek, D. G., Li, L. O., and Coleman, R. A. (2006) *J. Lipid Res.* **47,** 2004–2010
43. Ellis, J. M., Li, L. O., Wu, P. C., Koves, T. R., Ilkayeva, O., Stevens, R. D., Watkins, S. M., Muoio, D. M., and Coleman, R. A. (2010) *Cell Metab.* **12,** 53–64
44. Bu, S. Y., and Mashek, D. G. (2010) *J. Lipid Res.* **51,** 3270–3280
45. Askari, B., Kanter, J. E., Sherrid, A. M., Golej, D. L., Bender, A. T., Liu, J., Hsueh, W. A., Beavo, J. A., Coleman, R. A., and Bornfeldt, K. E. (2007) *Diabetes* **56,** 1143–1152
46. Durgan, D. J., Smith, J. K., Hotze, M. A., Egbejimi, O., Cuthbert, K. D., Zaha, V. G., Dyck, J. R., Abel, E. D., and Young, M. E. (2006) *Am. J. Physiol. Heart Circ. Physiol.* **290,** H2480–2497
47. Li, Z. Z., Berk, M., McIntyre, T. M., and Feldstein, A. E. (2009) *J. Biol. Chem.* **284,** 5637–5644
48. Miyazaki, M., Kim, Y. C., and Ntambi, J. M. (2001) *J. Lipid Res.* **42,** 1018–1024
49. Man, W. C., Miyazaki, M., Chu, K., and Ntambi, J. (2006) *J. Lipid Res.* **47,** 1928–1939
50. Miyazaki, M., Flowers, M. T., Sampath, H., Chu, K., Otzelberger, C., Liu, X., and Ntambi, J. M. (2007) *Cell Metab.* **6,** 484–496
51. Flowers, J. B., Rabaglia, M. E., Schueler, K. L., Flowers, M. T., Lan, H., Keller, M. P., Ntambi, J. M., and Attie, A. D. (2007) *Diabetes* **56,** 1228–1239
52. Borradaile, N. M., Han, X., Harp, J. D., Gale, S. E., Ory, D. S., and Schaffer, J. E. (2006) *J. Lipid Res.* **47,** 2726–2737
53. Borradaile, N. M., Buhman, K. K., Listenberger, L. L., Magee, C. J., Morimoto, E. T., Ory, D. S., and Schaffer, J. E. (2006) *Mol. Biol. Cell* **17,** 770–778
54. Back, S. H., Scheuner, D., Han, J., Song, B., Ribick, M., Wang, J., Gildersleeve, R. D., Pennathur, S., and Kaufman, R. J. (2009) *Cell Metab.* **10,** 13–26
55. Lin, J., Yang, R., Tarr, P. T., Wu, P. H., Handschin, C., Li, S., Yang, W., Pei, L., Uldry, M., Tontonoz, P., Newgard, C. B., and Spiegelman, B. M. (2005) *Cell* **120,** 261–273
56. Listenberger, L. L., Han, X., Lewis, S. E., Cases, S., Farese, R. V., Jr., Ory, D. S., and Schaffer, J. E. (2003) *Proc. Natl. Acad. Sci. U.S.A.* **100,** 3077–3082
57. Feldstein, A. E., Werneburg, N. W., Canbay, A., Guicciardi, M. E., Bronk, S. F., Rydzewski, R., Burgart, L. J., and Gores, G. J. (2004) *Hepatology* **40,** 185–194
58. Listenberger, L. L., Ory, D. S., and Schaffer, J. E. (2001) *J. Biol. Chem.* **276,** 14890–14895
59. Wei, Y., Wang, D., Topczewski, F., and Pagliassotti, M. J. (2006) *Am. J. Physiol. Endocrinol. Metab.* **291,** E275–E281
60. Cho, H. P., Nakamura, M., and Clarke, S. D. (1999) *J. Biol. Chem.* **274,** 37335–37339
61. Cho, H. P., Nakamura, M. T., and Clarke, S. D. (1999) *J. Biol. Chem.* **274,** 471–477
62. Stukey, J. E., McDonough, V. M., and Martin, C. E. (1990) *J. Biol. Chem.* **265,** 20144–20149
63. Mitchell, A. G., and Martin, C. E. (1995) *J. Biol. Chem.* **270,** 29766–29772
64. Hirono, H. (1983) *Tohoku J. Exp. Med.* **140,** 391–394
65. Hirono, H. (1984) *Lipids* **19,** 60–63
66. Rao, G. A., Manix, M., and Larkin, E. C. (1980) *Lipids* **15,** 55–60
67. Strittmatter, P., Thiede, M. A., Hackett, C. S., and Ozols, J. (1988) *J. Biol. Chem.* **263,** 2532–2535
68. Shanklin, J., Whittle, E., and Fox, B. G. (1994) *Biochemistry* **33,** 12787–12794
69. Pigeon, C., Legrand, P., Leroyer, P., Bouriel, M., Turlin, B., Brissot, P., and Loréal, O. (2001) *Biochim. Biophys. Acta* **1535,** 275–284
70. Goren, M. A., and Fox, B. G. (2008) *Protein Expr. Purif.* **62,** 171–178